Draft version April 14, 2005
Preprint typeset using LaTeX style emulateapj v. 11/26/04

INTERNAL SHOCKS IN THE MAGNETIC RECONNECTION JET IN SOLAR FLARES: MULTIPLE FAST SHOCKS CREATED BY THE SECONDARY TEARING INSTABILITY

S. Tanuma[1] & K. Shibata[1]

Draft version April 14, 2005

ABSTRACT

Space solar missions such as *Yohkoh* and *RHESSI* observe the hard X- and gamma-ray emission from energetic electrons in impulsive solar flares. Their energization mechanism, however, is unknown. In this paper, we suggest that the internal shocks are created in the reconnection jet and that they are possible sites of particle acceleration. We examine how magnetic reconnection creates the multiple shocks by performing two-dimensional resistive magnetohydrodynamic simulations. In this paper, we use a very small grid to resolve the diffusion region. As a result, we find that the current sheet becomes thin due to the tearing instability, and it collapses to a Sweet-Parker sheet. The thin sheet becomes unstable to the secondary tearing instability. Fast reconnection starts by the onset of anomalous resistivity immediately after the secondary tearing instability. During the bursty, time-dependent magnetic reconnection, the secondary tearing instability continues in the diffusion region where the anomalous resistivity is enhanced. As a result, many weak shocks are created in the reconnection jet. This situation produces turbulent reconnection. We suggest that multiple fast shocks are created in the jet and that the energetic electrons can be accelerated by these shocks.

Subject headings: acceleration of particles – Sun: flares – Sun: corona – MHD – plasmas – turbulence

1. INTRODUCTION

In impulsive flares, strong hard X-ray emission from energetic electrons has been observed by *Yohkoh* HXT (Masuda et al. 1994; see also a review by Miller et al. 1997). The origin of energetic electrons is, however, unknown. The fast-mode shock is known to be a possible site for particle acceleration, for example in interplanetary space (Terasawa & Scholer 1989) and supernova remnants (Blandford & Ostriker 1980; Koyama et al. 1995). To solve the particle acceleration problem in solar flares, Tsuneta & Naito (1998) suggested a diffusive shock model at the loop top. This model, however, has not yet been fully examined.

Solar flares occur as a result of magnetic reconnection. The SXT and HXT on the *Yohkoh* satellite discovered various pieces of evidence of magnetic reconnection (Tsuneta et al. 1992; Masuda et al. 1994; see review by Shibata 1999). The "fast" reconnection process suggested by Petschek (1964) can be supported by a localized resistivity (e.g, anomalous resistivity; Ugai 1986; Tanuma et al. 2003; see also Shibata, Nozawa, & Matsumoto 1992; Miyagoshi & Yokoyama 2003). Recently, Tanuma et al. (1999, 2001) investigated the reconnection triggered by a shock wave from a point explosion. They found that Petschek reconnection occurs immediately after the "secondary tearing instability" (Furth, Killeen, & Rosenbluth 1963; see also Magara & Shibata 1999; Shibata & Tanuma 2001), and that fast shocks are created in the reconnection jet. In this paper, we suggest that energetic electrons could be accelerated if the internal fast shocks could be created in solar flares (figure 1). To examine this possibility, we study how the internal shocks are created in the reconnection jet by performing 2D simulations with high spatial resolution. This should remove the effect of numerical noise and resolve the diffusion region.

These simulations lead us to propose that multiple fast shocks are created in solar flares and they are possible sites of particle acceleration. Our simulation method is described in the next section. In section 3, we present the simulation results. Finally, we discuss the results.

[1] Kwasan Observatory, Kyoto University, Yamashina, Kyoto, 607-8471, Japan: tanuma@kwasan.kyoto-u.ac.jp, shibata@kwasan.kyoto-u.ac.jp

2. MODEL OF NUMERICAL SIMULATIONS

We solve the nonlinear, time-dependent, resistive, compressible MHD equations. A rectangular computation box with 2D Cartesian coordinates in the x-z plane is assumed, where the x and z axes are in the horizontal and vertical directions, respectively. We assume an ideal gas, i.e., $p_g = (\gamma - 1)e$, where γ is the specific heat ratio (=5/3). The velocity and magnetic field are $\boldsymbol{v} = (v_x, v_z)$ and $\boldsymbol{B} = (B_x, B_z)$. Gravity is neglected.

In the initial equilibrium conditions, a Harris current sheet is assumed, i.e., $\boldsymbol{B}(x,z) = B_0 \tanh(z/l^{\rm init})\boldsymbol{x}$, $p_g(x,z) = p_{g0} + (B_0^2/8\pi)[1 - \tanh^2(z/l^{\rm init})]$, $\rho(x,z) = (\gamma p_g/T) = \rho_0 + (\gamma/T_0)(B_0^2/8\pi)[1 - \tanh^2(z/l^{\rm init})]$, where B_0, p_{g0}, and ρ_0, are dimensionless variables, and $\boldsymbol{x} = (1,0)$. We assume in the initial conditions that the current-sheet half-thickness $l^{\rm init} = 1$. The ratio of gas to magnetic pressure is $\beta = 8\pi p_{g0}/B_0^2 = 0.2$ ($|z| \gg l^{\rm init}$). The initial gas pressure is p_{g0} outside the current sheet, and $p_{g0} + B_0^2/8\pi = p_{g0}(1 + 1/\beta)$ inside the current sheet. The total pressure is uniform. We assume $p_{g0} = 1/\gamma = 0.6$ and $\rho_0 = 1$. The sound velocity and temperature are $C_s \equiv (\gamma p_g/\rho)^{1/2} = 1$ (uniform) and $T = T_0 = 1$ (uniform). The initial Alfvén velocity is $v_{\rm A}^{\rm init} = B_0/(4\pi\rho_0)^{1/2} \simeq 2.45$ ($|z| \gg l^{\rm init}$). We assume an anomalous resistivity model as follows: $\eta = \eta_0$ for

$v_d \le v_c$, and $\eta = \eta_0 + \alpha(v_d/v_c - 1)^2$ for $v_d > v_c$ (Kliem, Karlický, & Benz 1998; Ugai 1986; Tanuma et al. 1999, 2001), where $v_d (\equiv J/\rho)$, ρ, J, and v_c are the relative ion-electron drift velocity, mass density, current density, and threshold above which the anomalous resistivity sets in (Anomalous resistivity originates from a lower hybrid instability, ion-acoustic instability, or ion-cyclotron instability; see, e.g., Treumann 2001). We also assume that the resistivity does not exceed $\eta_{\max} = 1$. In this paper, we assume a "background resistivity" $\eta_0 = 0.005$, which is sufficiently larger than the "numerical resistivity" because of the grid size (Ugai 1999; Tanuma et al. 2001). The other parameters are $\alpha = 10.0$ and $v_c = 20.0$. We neglect the thermal radiation and heat conduction. They do not affect the basic properties of magnetic reconnection (Yokoyama & Shibata 1997).

We normalize the velocity, length, and time by the sound velocity (C_s), initial current-sheet thickness (H), and H/C_s, respectively. The units of normalization are $C_s \sim 150$ km s^{-1}, $H \sim 3000$ km, and $\tau \equiv H/C_s \sim 20$ s. The units of temperature, density, gas pressure, and magnetic field strength are $T_0 \sim 2 \times 10^6$ K, $n_0 \sim 10^9$ cm^{-3}, $p_{g0} \sim 10^{-1}$ erg cm^{-3}, and $B_0 \sim 2$ G, respectively (B_0 is ~ 10 G if we assume $n_0 \sim 2.5 \times 10^{10}$ cm^{-3}). The grid number is $(N_x, N_z) = (13000, 1300)$, and the grid size is uniform $(\triangle x, \triangle z) = (0.013, 0.013)$. We assume that the top ($z = +8.45$) and bottom ($z = -8.45$) surfaces are free boundaries, and that the right ($x = +84.5$) and left ($x = -84.5$) ones are periodic. The simulation box size is $(L_x, L_z) = (169.0, 16.9)$. The magnetic Reynolds number is $\mathrm{Re}_m^{\mathrm{init}} \equiv v_{\mathrm{A}}^{\mathrm{init}} L_x/\eta_0 \sim 84500$. We use a 2-step modified Lax-Wendroff method. The resistivity is initially enhanced for a short time in the central region of the current sheet (see also Ugai 1986).

3. RESULTS

Figure 2 shows the time variation of the spatial distribution of the gas pressure in the reconnection region. The current sheet is unstable because of the tearing instability (Furth et al. 1963). The magnetic dissipation time, Alfvén time, and tearing instability time scale are $\tau_{\mathrm{dis}}^{\mathrm{init}} = {l^{\mathrm{init}}}^2/\eta_0 \sim 200$, $\tau_{\mathrm{A}}^{\mathrm{init}} = l^{\mathrm{init}}/v_{\mathrm{A}}^{\mathrm{init}} \sim 0.4$, and $\tau_t^{\mathrm{init}} = (\tau_{\mathrm{dis}}^{\mathrm{init}} \tau_{\mathrm{A}}^{\mathrm{init}})^{1/2} \sim 9$, respectively, where $l^{\mathrm{init}} (= 1)$ is the half thickness of the initial current sheet. The tearing instability is initiated in the current sheet by the initial perturbation. The current sheet becomes gradually thinner in the nonlinear phase of the tearing instability ($t \sim 7 - 18$). Its length is comparable to the most unstable wavelength of the tearing instability, i.e., $\lambda_t \sim 5.6 {\mathrm{Re}_{m,z}^{\mathrm{init}}}^{1/4} l^{\mathrm{init}}$ (Magara & Shibata 1997; Tanuma et al. 2001), where $\mathrm{Re}_{m,z}^{\mathrm{init}} \equiv v_{\mathrm{A}}^{\mathrm{init}} l^{\mathrm{init}}/\eta_0 \sim 500$. λ_t is ~ 25 in this simulation. The current-sheet thickness in this phase is $l_t \sim (\lambda_t/2) \mathrm{Re}_{m,t}^{-1/2}$, i.e., the current sheet corresponds to that of a Sweet(1958)-Parker(1957) sheet. The magnetic Reynolds number is $\mathrm{Re}_{m,t} = (\lambda_t/2) v_{\mathrm{A}}^{\mathrm{init}}/\eta_0$ in this phase. Furthermore, $\mathrm{Re}_{m,t} \sim 6000$ and $l_t \sim 0.15$. These values explain our results well.

The sheet becomes very long so that it becomes unstable to the tearing instability again at $t \sim 17-78$ (referred to as the "secondary tearing instability" in Tanuma et al. 1999, 2001). The secondary tearing instability starts just after the Sweet-Parker sheet is created on a time scale of $\tau_{2t} = ({l_t}^3/\eta_0 v_{\mathrm{A}}^{\mathrm{init}})^{1/2} \sim 0.52$. The drift velocity ($v_d$) reaches a threshold ($v_c$) at $t \sim 18$ so that anomalous resistivity sets in. v_d, however, remains a little larger than v_c when $18 < t < 20$. Figure 3a shows that the magnetic islands are actually created at the diffusion region (But plasmoids are difficult to represent clearly in figure 2a). The gaps between them ($\sim 0.3 - 0.5$) are not consistent with the analytic solution of the secondary tearing instability in this model, $\lambda_{2t} \sim 4.9 {\mathrm{Re}_{m,z}^{2t}}^{1/4} l_t$, where $\mathrm{Re}_{m,z}^{2t} = v_{\mathrm{A}}^{\mathrm{init}} l_t/\eta_0$, $\lambda_{2t} \sim 2.2$, and $\mathrm{Re}_{m,z}^{2t} \sim 73.5$, respectively. The current-sheet thickness becomes $l_{2t} = {\mathrm{Re}_m^{2t}}^{-1/2} (\lambda_{2t}/2) \sim 0.047$, where the magnetic Reynolds number is $\mathrm{Re}_m^{2t} = (\lambda_{2t}/2) v_{\mathrm{A}}^{\mathrm{init}}/\eta_0 = 539$. This is because the analytic solution is in the large Re_m approximation regime.

The drift velocity increases a great deal above the threshold at $t \sim 20$ before the current sheet completes its collapse to a thickness of l_{2t}. Because of the excitation of anomalous resistivity, non-steady Petschek(1964)-like (fast) reconnection starts, and is accompanied by slow shocks. During fast reconnection ($t > 20$), the secondary tearing instability occurs in the dissipation region where the anomalous resistivity is enhanced. This diffusion region is well resolved numerically. The magnetic Reynolds number is now $\mathrm{Re}_{m,z}^{2t*} = v_{\mathrm{A}}^{\mathrm{init}} l_t/\eta_{\max} \sim 0.38$. The wavelength and time scale of the secondary tearing instability are $\lambda_{2t}^* \sim 4.9 {\mathrm{Re}_{m,z}^{2t*}}^{1/4} l_t \sim 0.58$ and $\tau_{2t}^* = ({l_t}^3/\eta_{\max} v_{\mathrm{A}}^{\mathrm{init}})^{1/2} \sim 0.0014$, respectively, provided we assume that the secondary tearing instability starts when $l \sim l_t$. Figure 3b also shows that the plasmoids are created at this time. Their wavelengths are consistent with the above theoretical value. This result can be explained by extension of the results of Steinolfson & van Hoven (1983), although the analytic solution is in the large Re_m approximation regime. Due to the bursty, time-dependent reconnection, many weak shocks are created in the reconnection jet. They are almost stationary, when they are created outside the diffusion region, although they move inside and near the diffusion region. Figure 4 displays the profiles of some variables in $z = 0.058$, when $t = 35.0$. The profiles show that 12 weak shocks are created among $0 < x = 6.5$. Hence, the gaps between them ($\sim 6.5/12 \sim 0.54$) are quite consistent with λ_{2t}^* (Note that the local Alfvén velocity is smaller than $v_{\mathrm{A}}^{\mathrm{init}}$ during this phase). The reconnection jet can become supersonic and the pressure jumps are almost standing so that they could be shocks. The reconnection rate and inflow velocity toward the diffusion region oscillate. As a result, the reconnection becomes "turbulent" (Matthaeus & Lamkin 1985, 1986; Lazarian & Vishniac 1999; Fan, Feng, & Xiang 2004) during the late phase. In this phase, the Kelvin-Helmholtz instability may also occurs (see discussion).

We examine the dependence of the results on the plasma β and resistivity model (η_0, v_c, and α). These parameters do not affect our principal results; fast shocks are created in all simulations. For example, the physical values are $\mathrm{Re}_{m,z}^{\mathrm{init}} \sim 500 (l^{\mathrm{init}}/1.0)\ (\eta_0/0.005)^{-1}\ (\beta/0.2)^{-1/2}$, $\lambda_t \sim 25 (l^{\mathrm{init}}/1.0)^{5/4}\ (\eta_0/0.005)^{-1/4}\ (\beta/0.2)^{-1/8}$, and $l_t \sim 0.15 (l^{\mathrm{init}}/1.0)^{5/8}\ (\eta_0/0.005)^{3/8}\ (\beta/0.2)^{3/16}$, respectively. Furthermore, $\lambda_{2t}^* \sim 0.58 (l^{\mathrm{init}}/1.0)^{25/32}$

$(\eta_0/0.005)^{15/32}$ $(\eta_{\rm max}/1.0)^{-1/4}$ $(\beta/0.2)^{7/64}$, and $\tau_{2t}^* \sim 0.0014(l^{\rm init}/1.0)^{15/16}$ $(\eta_0/0.005)^{9/16}$ $(\eta_{\rm max}/1.0)^{-1/2}$ $(\beta/0.2)^{17/32}$, if anomalous resistivity is assumed to be excited to $\eta \sim \eta_{\rm max}$ when the current-sheet thickness is $l \sim l_t$. A detailed investigation of the parameter-dependence will be published elsewhere.

4. DISCUSSION

We suggest that bursty, time-dependent reconnection creates many weak shocks (plasmoids) in the reconnection jet, which could become multiple fast shocks in actual flares. Reconnection produces an outflow whose velocity is comparable with the local sound speed. Thus, it can create fast shocks which would provide sites for Fermi acceleration. From our numerical simulations, the number of energetic electrons can be determined by the flux into the internal shocks, and is calculated to be $dN/dt \sim 10^{35}$ s^{-1} (see also Tsuneta & Naito 1998). The reconnection site evolves in a self-similar manner (Nitta et al. 2001), so the evidence of bursty reconnection and internal shocks shown in this paper may be observed by the *Solar-B* satellite which will be launched in 2006. If the energetic electrons are accelerated in the fast shocks, the number of energetic electrons would increase with distance from the diffusion region.

Our simulations show that the reconnection jet ("downflow") produces turbulence. The turbulent field at the loop top helps to accelerate and confine the energetic electrons (Jakimiec et al. 1998). As a second important application, we suggest that the non-steady ejection of plasmoids can create the internal shocks. They actually appear in some of our simulations with different parameters, which we will examine in a future paper. This could explain the oscillations (Innes, McKenzie, & Wang 2003) and non-steady plasmoid ejections (McKenzie & Hudson 1999; Asai et al. 2004) in the downflows. In fact, some results with different parameters show the oscillation and multiple oblique shocks in the jet, which could be due to the Kelvin-Helmholtz instability (Biskamp, Schwarz, & Zeiler 1998; Tanuma 2000; Arzner & Scholer 2001; Tanuma & Shibata 2002, 2003b, 2004). Furthermore, spatial patterns that are similar to the multiple oblique shocks appear in galactic jets (e.g., Hardee et al. 1991).

The non-steady ejection and bow shock propagation can also play an important role in slowly drifting structures (Karlický 2003), and narrowband dm-spikes (Bárta & Karlický 2001) in the upward jet. The time scale for the tearing instability in the diffusion region is ~ 30 $(l/10^5$ cm$)^{3/2}$ $(v_{\rm A}/10^8$ cm s$^{-1})^{-1/2}$ $(T/10^6$ K$)^{3/4}$ s if we assume Spitzer conductivity and that the diffusion region thickness is l. This explains the time scales associated with the above phenomena (Karlický 2003). Our results can also be applied to particle acceleration in the Galactic plane (Tanuma & Shibata 2003a) etc.

The authors thank the anonymous referee for useful suggestions, which improved this work very much. One of the authors (S.T.) thanks M. Fujimoto, M. Hoshino, B. Kliem, K. Kondoh, Tohru Shimizu, A. Takeuchi, T. Terasawa, S. Tsuneta, M. Ugai, & T. Yokoyama for various fruitful discussions and comments. The authors also thank D. Brooks for brushing up this paper. Part of the numerical computations were carried out on the VPP5000 at the ADAC of the NAOJ (PI: S. Tanuma; project ID: mst21a, yst15a, rst03a). The other part was carried out on the VPP5000 at the ITC, Nagoya Univ., by the joint research program of the STEL, Nagoya University (PI: S. Tanuma). This work was partially supported by ACT-JST Cooperation (PI: R. Matsumoto), by the JSPS Japan-US Cooperation Science Program (PI: K. Shibata & K. I. Nishikawa), by the JSPS Japan-UK Cooperation Science Program (PI: K. Shibata & N. O. Weiss), and the Grant-in-Aid for the 21st Century COE "Center for Diversity and Universality in Physics" from the MEXT of Japan. S.T. is supported by a Grant-in-Aid for JSPS Fellows.

REFERENCES

Arzner, K. & Scholer, M. 2001, J. Geophys. Res., 106, 3827
Asai, A., Yokoyama, T., Shimojo, M., & Shibata, K. 2004, ApJ, 605, L77
Bárta, M. & Karlický, M. 2001, A&A, 379, 1045
Biskamp, D., Schwarz, E., & Zeiler, A. 1998, Phys. Plasmas, 5, 2485
Blandford, R. D. & Ostriker, J. P. 1980, ApJ, 237, 793
Fan, Q.-L., Feng, X.-S., & Xiang, C.-Q. 2004, Phys. Plasmas, 11, 5605
Furth, H. P., Killeen, J., & Rosenbluth, M. N. 1963, Phys. Fluid, 6, 459
Hardee, P. E., Norman, M. L., Coupelis, T., & Clarke, D. A. 1991, ApJ, 373, 8
Innes, D. E., McKenzie, D. E., & Wang, T. 2003, Sol. Phys., 217, 247
Jakimiec, J., Tomczak, M., Falewicz, R., Phillips, K. J. H., & Fludra, A. 1998, A&A, 334, 1112
Karlický, M. 2003, A&A, 417, 325
Kliem, B., Karlický, M., & Benz, A. O. 2000, A&A, 360, 715
Koyama, K., Petre, R., Gotthelf, E. V., Hwang, U., Matsuura, M., Ozaki, M., & Holt, S. S. 1995, Nature, 378, 255
Lazarian, A., & Vishniac, E. T. 1999, ApJ, 517, 700
Magara, T. & Shibata, K. 1999, ApJ, 514, 456
Masuda, S., Kosugi, T., Hara, H., Tsuneta, S., & Ogawara, Y. 1994, Nature, 371, 495
Matthaeus, W. H. & Lamkin, S. L. 1985, Phys. Fluids, 28, 393
Matthaeus, W. H. & Lamkin, S. L. 1986, Phys. Fluids, 29, 2513
McKenzie, D. E. & Hudson, H. S. 1999, ApJ, 519, L93
Miller, J. A. et al. 1997, J. Geophys. Res., 102, 14631
Miyagoshi, T. & Yokoyama, T. 2003, ApJ, 593, L133
Nitta, S., Tanuma, S., Shibata, K., & Maezawa, K. 2001, ApJ, 550, 1119
Parker, E. N. 1957, J. Geophys. Res., 62, 509
Petschek, H. E. 1964, in the Physics of Solar Flares, the AAS-NASA Symp. on the Physics of Solar Flares, ed. W. N. Hess (Washington DC: NASA), 425
Shibata, K., Nozawa, S., & Matsumoto, R. 1992, PASJ, 44, 265
Shibata, K. 1999, Ap&SS, 264, 129
Shibata, K. & Tanuma, S. 2001, Earth, Planets & Space, 53, 473
Steinolfson, R. S. & van Hoven, G. 1983, Phys. Plasmas, 26, 117
Sweet, P. A. 1958, in Electromagnetic Phenomena in Cosmical Physics, IAU Symp. 6, ed. B. Lehnert (Kluwer Academic Publishers: Dordrecht), 123
Tajima, T. & Shibata, K. 1997, Plasma Astrophysics (Addison and Wesley: Reading)
Tanuma, S. 2000, PhD thesis, University of Tokyo, p106
Tanuma, S. & Shibata, K. 2002, in the IAU 8th IAU Asia-Pacific Regional Meeting, Vol II, ed. S. Ikeuchi, J. Hearnshaw, & T. Hanawa (Tokyo: ASJ), 469
——. 2003a, in Proc. of the 28th Intl. Cosmic Ray Conf.: ICRC 2003, ed. T. Kajita et al. (Universal Academy Press: Tokyo), 2277

——. 2003b, in Proc. of the 28th Intl. Cosmic Ray Conf.: ICRC 2003, ed. T. Kajita et al. (Universal Academy Press: Tokyo), 3351
——. 2004, in Multi-Wavelength Investigations of Solar Activity, IAU Symp. 223, ed. A.V. Stepanov, E. E. Benevolenskaya, & A. G. Kosovichev, (Cambridge University Press), in press
Tanuma, S., Yokoyama, T., Kudoh, T., Matsumoto, R., Shibata, K., & Makishima, K. 1999, PASJ, 51, 161
Tanuma, S., Yokoyama, T., Kudoh, T., & Shibata, K. 2001, ApJ, 551, 312
——. 2003, ApJ, 582, 215
Terasawa, T. & Scholer, M. 1989, Science, 244, 1050
Treumann, R. A. 2001, Earth, Planets & Space, 53, 453
Tsuneta, S., Hara, H., Shimizu, T., Acton, L. W., Strong, K. T., Hudson, H. S., & Ogawara, Y. 1992, PASJ, 44, L63
Tsuneta, S. & Naito, T. 1998, ApJ, 495, L67
Ugai, M. 1986, Phys. Fluids, 29, 3659
Ugai, M. 1999, Phys. Plasma, 6, 1522
Yokoyama, T. & Shibata, K. 1997, ApJ, 474, L61

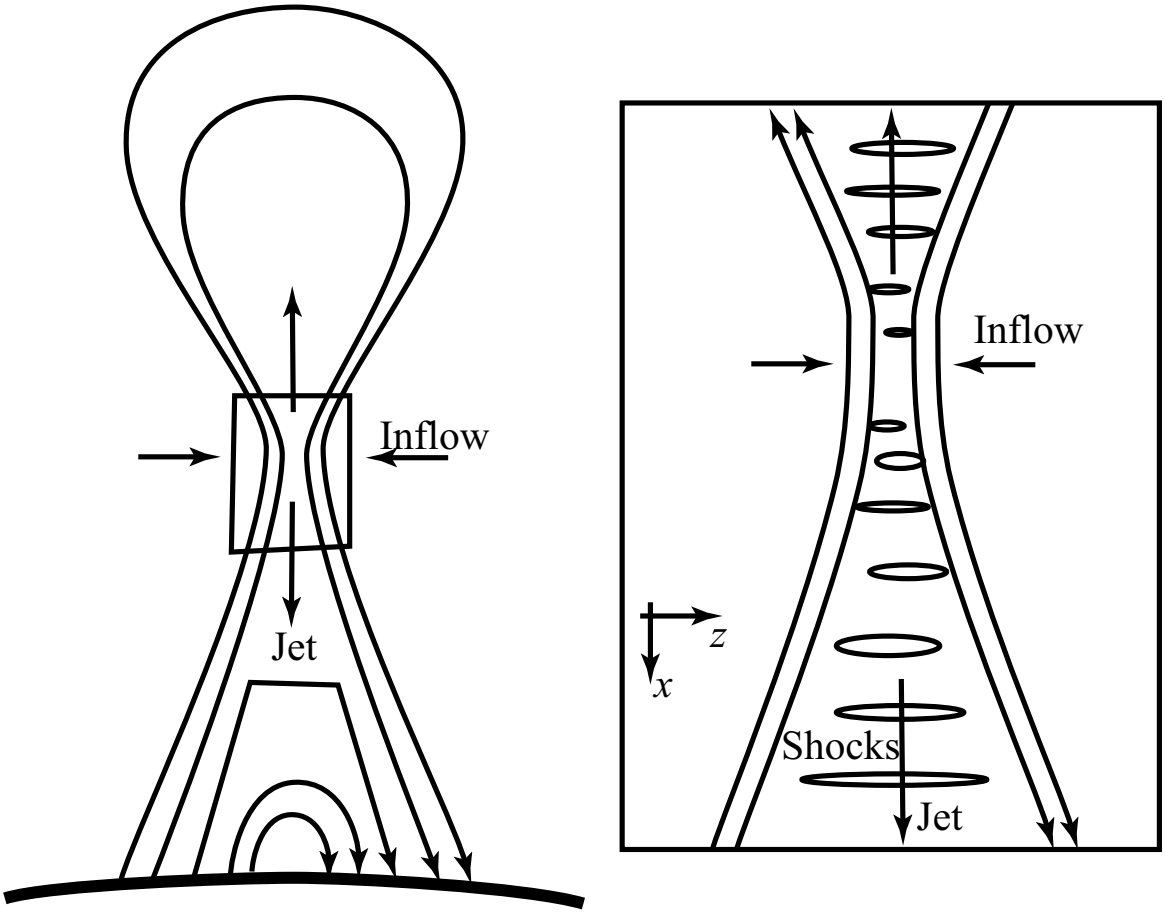

FIG. 1.— Schematic illustration of the internal shocks in the reconnection jet in solar flares.

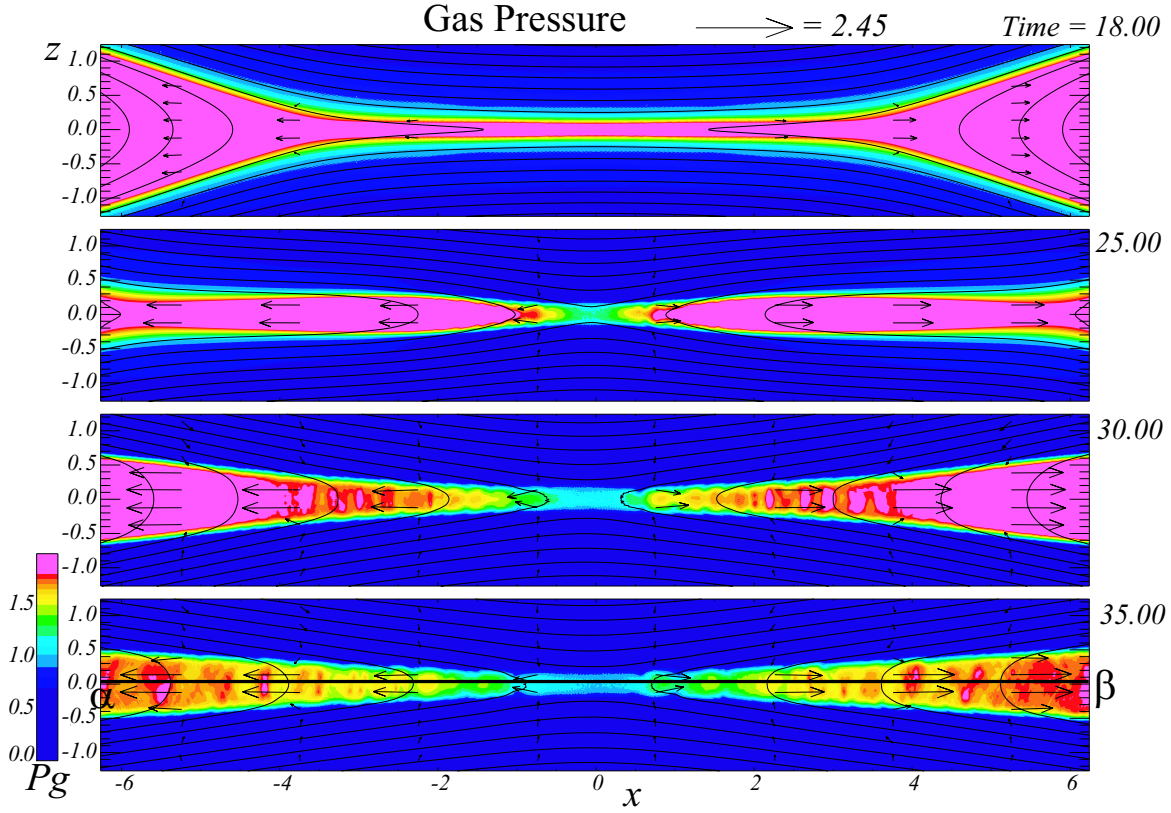

FIG. 2.— The gas pressure. The drift velocity reaches the threshold at $t \sim 18$. Petschek-like reconnection starts at $t \sim 20$. Bursty, time-dependent fast reconnection creates many weak shocks in the reconnection jet.

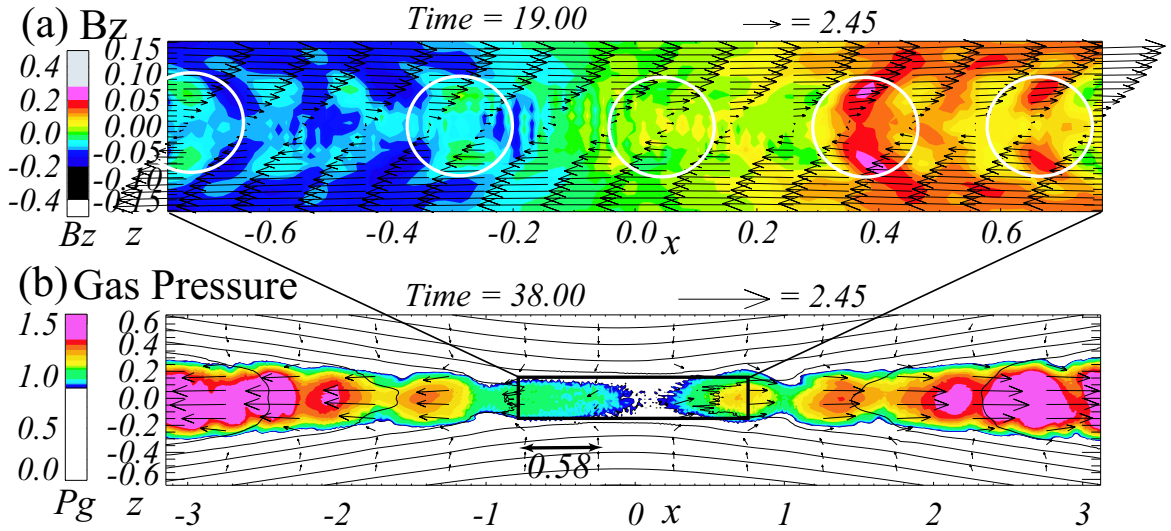

FIG. 3.— (a) B_z and $\boldsymbol{B}$ vectors in diffusion regions. The white circles indicate the large B_z regions. It shows that small magnetic islands are created, although their gas is smaller than the theoretical wavelength of the secondary tearing instability ($\lambda_{2t} \sim 2.2$). (b) The gas pressure and $\boldsymbol{v}$ vectors at the diffusion region. The gaps between the shocks are quite consistent with the theoretical value ($\lambda^*_{2t} \sim 0.58$; shown by the arrow).

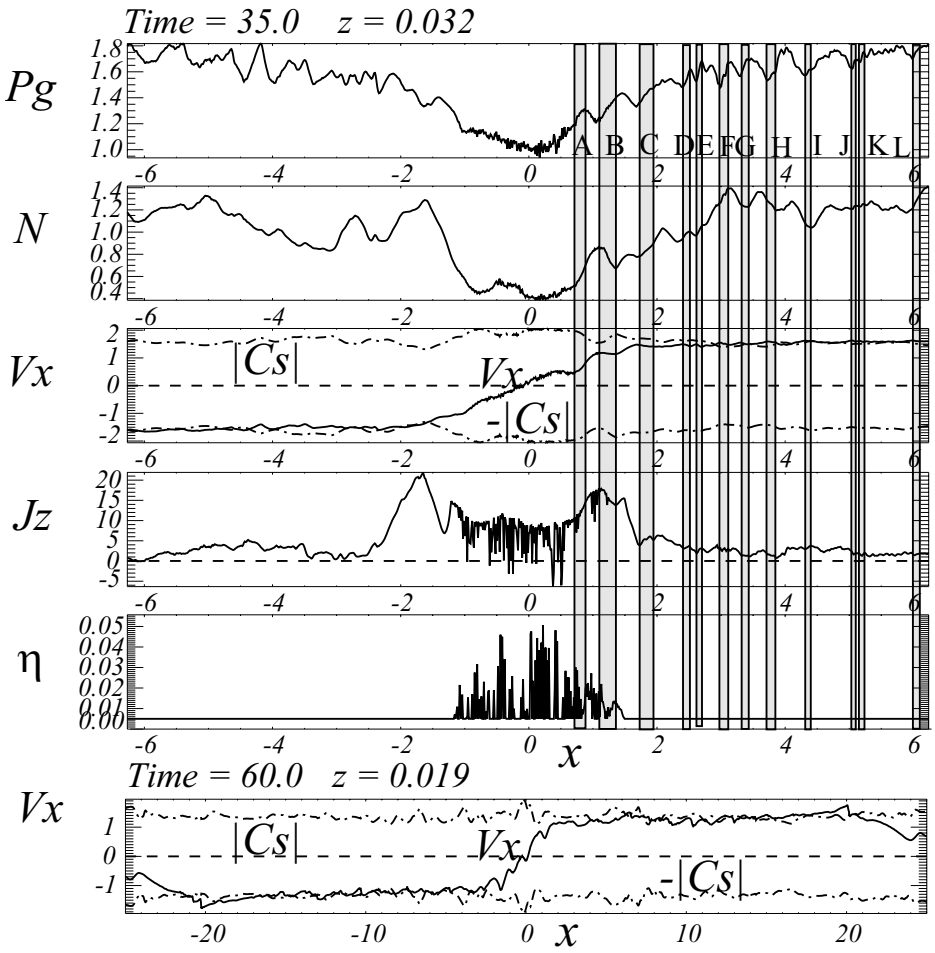

FIG. 4.— The profiles of some variables in $z = 0.032$ at $t = 35.0$ between 'α' and 'β' plotted in fig 2. Gray boxes show the pressure jumps created in the reconnection jet. They are almost standing shocks. The Rankine-Hugoniot relation is satisfied, for example, by more than 91 % at the jump named 'B'. In the 3rd plot, the local sound velocity (C_s) is also displayed by dashed-dotted lines. The velocity of jet is comparable with $|C_s|$ so that the jet can be supersonic and can be weak shocks. The pressure jumps are resolved by more than 10 grids. The bottom plot is same with 3rd one but in $z = 0.025$ at $t = 60$.